Functional Nanocomposites Formation by Electrochemical Deposition of Metals and Semiconductors into Porous Silicon

E.B. Chubenko[1,*], A.L. Dolgiy[1], S.V. Redko[1], A.I. Sherstnyov[1], K.I. Yanushkevich[2],
S.L. Prischepa[1], V.P. Bondarenko[1]

[1] *Belorussian State University of Informatics and Radioelectronics, 6, P. Brovki Str., 220013 Minsk, Belarus*
[2] *Scientific-Practical Materials Research Centre of NAS of Belarus, 19, P. Brovki Str., 220072 Minsk, Belarus*

The paper concerns the study of formation of nanocomposites by electrochemical deposition of metals and semiconductors into the porous silicon. Ni and ZnO were used as experimental materials for deposition. The influence of deposition process parameters and structure of initial porous silicon substrates on morphology and composition of formed metal or semiconductor nanostructures are studied. Obtained nanocomposites demonstrated high filling factor and uniformity. Porous silicon/Ni nanocomposites showed strong magnetic anisotropy. Porous silicon/ZnO nanocomposites after thermal annealing had intensive photoluminescence in the visible range. Applications of obtained nanocomposites in the magnetic and optoelectronic devices discussed as well.

1. INTRODUCTION

Porous silicon (PS) is a versatile material which can be used in electronics, photovoltaics and medicine [1]. Due to regular structure of vertically oriented pores with uniform diameter distribution it can be used as a host material for fabrication of nanostructure arrays or nanocomposites [2]. In this case PS can play a role of passive matrix containing regular array of nanowires (NW) of different material deposited into the pores [2 – 4]. Material in the form of nanowires can exhibit properties different from that of same material in the bulk due to the quantum confinement effects. In nanocomposite both silicon and introduced material defines its properties which can be presented as a combination or superposition of individual properties of nanocomposite components [2, 3].

One of the issues of fabrication of PS based nanocomposite materials is the difficulty of introducing other material into the pores. Each pore is a high aspect ratio tube with a nanometric size diameter and length up to several micrometers [1]. Many standard microelectronic techniques such as CVD, MBE, magnetron sputtering allow to deposit materials only on the top of PS layer [1, 2]. The reason of such behavior is that media from which precipitation occurs remains "outside" of pores. More useful approach is the deposition from liquid phase, for example, by electrochemical or chemical methods [4, 5]. Solution can penetrate the whole porous structure providing the deposition along the full length of the pores [6, 7]. However the deposition process may be complicated by capillary effects and nonuniformity of porous structure [8].

The aim of this work is the fabrication of nanocomposites by electrochemical deposition of metals and semiconductors into PS with improved uniformity by variation of deposition process parameters and structure of initial PS templates.

2. EXPERIMENTAL

The n-type antimony-doped (100)-oriented Si wafers with resistance of 0.01 Ω·cm were used to fabricate the PS matrix template. The formation of PS was carried out in galvanostatic and pulsed galvanostatic mode in the dark. 9 % HF solution with 20 % of isopropanol was used for galvanostatic silicon anodisation at current density $10 - 100$ mA/cm^2. The formation of PS in pulsed galvanostatic mode was carried out in 9 % HF aqueous electrolyte. Each cycle consisted of 1 s positive anodisation pulse and 4.5 s relaxation period. Current density of anodisation pulse was $20 - 120$ mA/cm^2.

Nickel was incorporated into the PS template by electrochemical galvanostatic deposition at constant current density of 3.5 mA/cm^2. The composition of electrolyte for Ni deposition consisted of 213 g/l NiSO$_4$, 5 g/l NiCl$_2$, 25 g/l H$_3$BO$_3$ and 3 g/l saccharin. pH of the solution was 2.6 at 20 °C. Ni was deposited into PS templates for 60 min at room temperature.

ZnO cathodic electrochemical deposition was carried out in DMSO based solutions containing 0.03 M ZnCl$_2$ and 0.1 M KCl, and also different amount of polyoxyethylene (POE) and H$_2$O$_2$. ZnO was deposited at current density of $0.3 - 0.5$ mA/cm^2 at 100 °C during 60 min.

All samples after deposition were rinsed and dried on air.

3. RESULTS AND DISCUSSIONS

3.1 PS/Ni nanocomposites

The optimal porosity (70 %) and pore size of PS template for Ni deposition was obtained in galvanostatic mode at current density of 80 mA/cm^2.

Fig. 1 presents scanning electron microscopy (SEM) cross sections images of the PS layer with Ni NWs. Pore channels in this case are well filled with metal.

NWs represent columns of the large tightly contacted conglomerates of Ni. In the top part of PS coalesced Ni particles are observed.
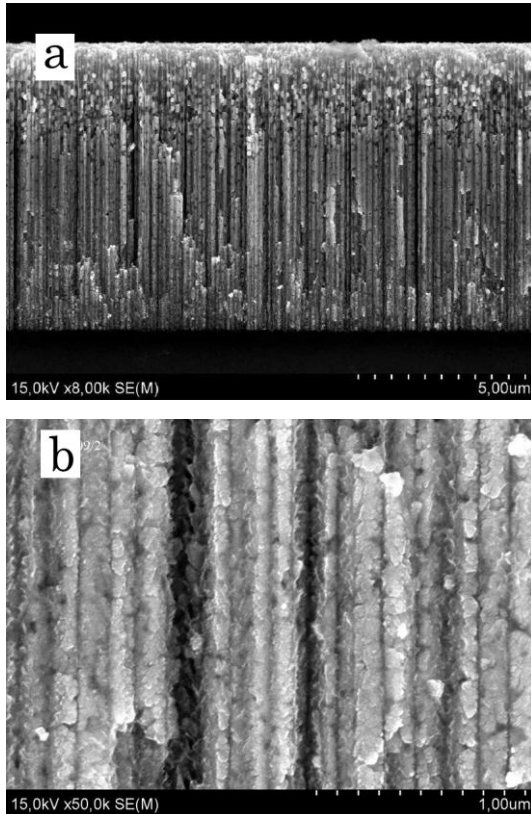

Fig. 1 – SEM images of the whole cross section (a) and middle part (b) of the PS/Ni nanocomposite

The diameter of the particles varies in the range from 100 to 120 nm. It exactly corresponds to the diameters of the pore channels. The thickness of PS layer used for Ni deposition was 10 µm. It should be noted that pretreatment of the sample, resulting in the exfoliation of the surface layer of Ni, could destroy the Ni NWs in the upper part of the sample. In the middle of the sample nickel NWs are rather monolithic. At the bottom of sample the completeness of nickel filling is lower than in the central part. It is possible to see the individual NPs of nickel. The filling factor was estimated as 67 %.

For the ferromagnetic resonance (FMR) study the spectrometer of electronic paramagnetic resonance (EPR) "RadioPAN Se/X-2543" in X–band on the frequency f = 9.32 GHz was used. The polarized magnetic field was modulated with the frequency f = 100 kHz and amplitude $\Delta B = 0.1$ mT. The resonance measurements were performed at room temperature at dark on air. The orientation of the samples in the external magnetic field was characterized by the polar angle Θ_B between the magnetic induction B and normal to surface of the sample. The value of the resonant magnetic induction B_r depends on the orientation of the magnetic field with respect to the NWs axis, which indicates the presence of the ferromagnetic resonance. The peak to peak widths of the measured curves are $\Delta B_{pp} = 110$ mT at $\Theta_B = 0°$ and $\Delta B_{pp} = 135$ mT at $\Theta_B = 90°$. Such meas-

urements were performed at different Θ_B values. The original FMR spectra in the range $0° \le \Theta_B \le 90°$ are shown in the Fig. 2.
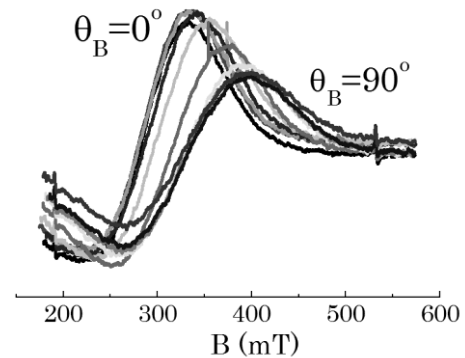

Fig. 2 – Measured FMR spectra of arrays of Ni NWs in PS for different values of Θ_B. From left to right, $\Theta_B = 0°$; 10°; 15°; 30°; 45°; 60°; 75°; 80°; 85°; 90°

On the base of the measured FMR spectra it is possible to plot the dependence of the resonance field B_r on the angle Θ_B. This result is shown in the Fig. 3. The obtained angular dependence of B_r indicates the presence of the easy axis magnetic anisotropy, which coincides with the axes of Ni NWs.
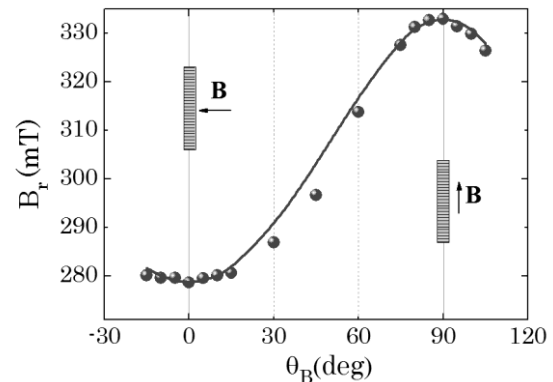

Fig. 3 – Dependence of the resonant magnetic inductance B_r on the angle Θ_B for the arrays of Ni NWs in PS

The isothermal M(H) dependences were measured using a MPMS SQUID-VSM magnetometer. The magnetic moment was measured with the sensitivity of 10^{-8} emu. Magnetic field was applied either parallel (out of plane configuration (OOP, $\Theta_B = 0°$), or perpendicular (in plane configuration (IP, $\Theta_B = 90°$)) to the Ni NWs axis. The magnetization curves, recorded for OOP and IP configurations at two temperatures (T = 5 K and 300 K), are presented in the Fig. 4. The evolution of the magnetic hysteresis loops shows a narrowing tendency towards higher temperatures.

It can be seen that the easy axis anisotropy dominates for the OOP configuration, which coincides with the results of the FMR study (Fig. 3).
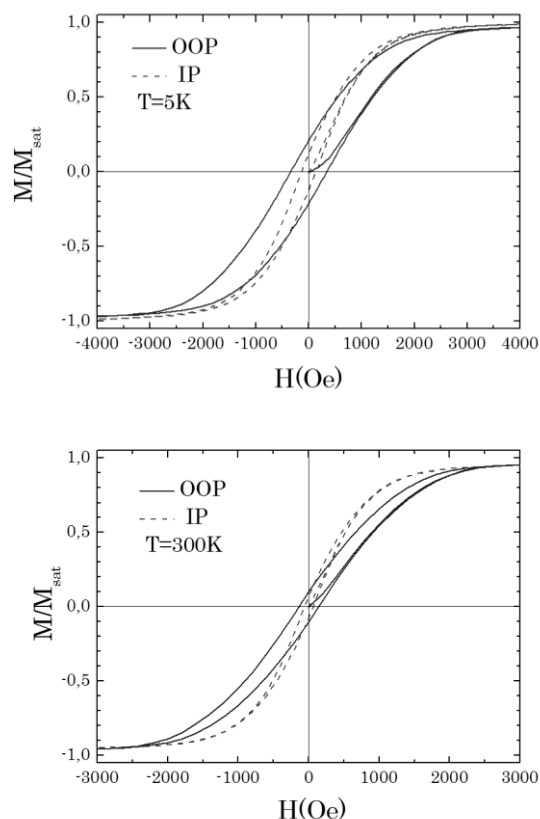
Fig. 4 – Field dependence of the normalized magnetization $M=M_{sat}$ for arrays of Ni NWs in PS

By analyzing the angular dependence of the resonant magnetic filed at f = 9.32 GHz for arrays of Ni NWs in PS we observed a uniaxial anisotropy with easy axis oriented along the Ni NWs. This result was confirmed from magnetostatic measurements at different temperatures.

3.2 PS/ZnO nanocomposites

For ZnO deposition PS templates formed in a pulsed galvanostatic mode were used due to the uniformity of their structure. During the investigation of formation of PS in a pulsed galvanostatic mode it was found that PS formed at current density above 90 mA/cm² has more regular structure with smooth pore walls and demonstrates no branching. The optimal current density of PS formation was approximately 120 mA/cm². At higher current densities the top parts of the silicon crystallites begin to chemically dissolve in the aqueous HF solution. At lower current densities minor branching is still observed. The thickness of PS matrix used for ZnO deposition was 10 µm.

Deposition of ZnO from the DMSO solution with and without POE at the same current density revealed that presence of the high order polymer inhibit electrochemical reactions of ZnO formation on the surface of PS therefore preventing pore mouths closing. The latter effect interfere the electrolyte circulation along and in/out of the pores and therefore blocks deposition of the ZnO in the depth of the pore and make their complete filling impossible.

On the Fig. 5 cross-sections of the PS/ZnO nanocomposite with ZnO deposited from the POE containing solution at 0.5 mA/cm². Deposited ZnO nanoparticles have hexagonal shape and average diameter 50 nm. ZnO crystal distribution along the PS pores is more uniform with larger concentration at the bottom and lower concentration at the top part compared to the samples obtained with the solutions without POE at the same current density.
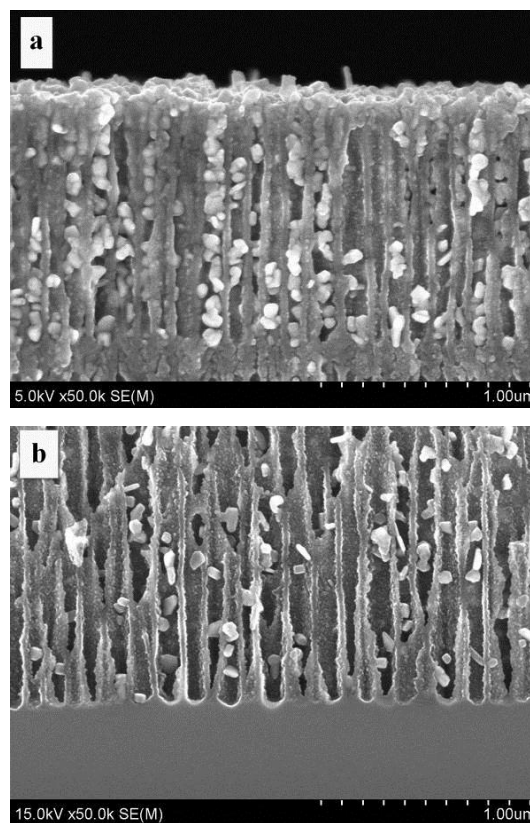

Fig. 5 – SEM images of the top (a) and bottom (b) parts of cross-section of PS/ZnO nanocomposite. ZnO was deposited at 0.5 mA/cm² in the POE containing solution

However it was found that at lower current density of 0.3 mA/cm² pore openings are not closed with ZnO crystals even without POE. But ZnO deposition rate decreasing results in the formation of fewer ZnO crystals of smaller size during the same period of time according to the Faraday's law (Fig. 6).

The study of composition of obtained PS/ZnO nanocomposites by EDS analysis revealed that at higher current density (0.5 mA/cm²) the excess of Zn is observed. It's typical for the case of dissolved oxygen atoms shortage in the solution and high negative deposition potentials at which metallic Zn deposition reactions occurs. After the addition of H_2O_2 to the solution the excess of O in the formed nanocomposite observed, i.e. it leads to formation of more stoichiometric ZnO (also confirmed by XRD spectra) and partial Si oxidation. At lower current density (< 0.3 mA/cm²) deposit has excess of O.
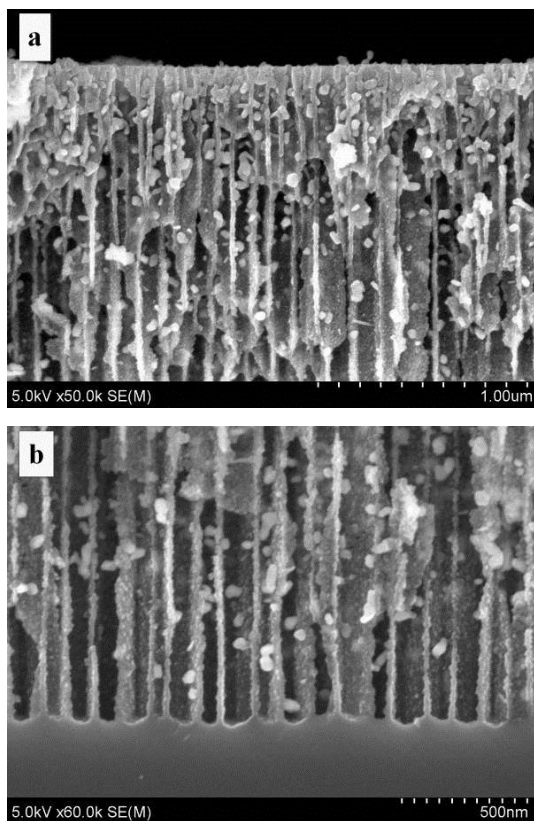
Fig. 6 – SEM images of the top (a) and bottom (b) parts of cross-section of PS/ZnO nanocomposite. ZnO was deposited at 0.3 mA/cm^2

Unannealed PS/ZnO nanocomposite samples do not show essential photoluminescence both in UV and visible ranges (Fig. 7) due to a small amount of deposited ZnO and opacity of unoxidized PS. After annealing for 1 h at 400 °C intensive complex photoluminescence band with two maximums at 600 and 660 nm appeared. These bands correspond to recombination processes via energy levels in ZnO bandgap related to oxygen defects in crystal lattice [9]. The photoluminescence became visible due to partial oxidation of PS skeleton. After annealing for 1 h at 900 °C photoluminescence spectra changed significantly. New bands with a maximum at 530 nm and 380 nm occurred. The first one can be associated with the presence of Zn vacancies in ZnO crystal lattice [9]. Band in a UV range corresponds to band-to-band recombination in ZnO [9].

Fig. 7 – Room temperature photoluminescence spectra of PS/ZnO nanocomposites after thermal annealing at different temperatures. Excitation wavelength – 340 nm

4. CONCLUSIONS

PS based nanocomposites obtained by electrochemical method have good uniformity and, particularly in the case of PS/Ni structures, high filling factor (up to 67 %). The key factors in the process of successful PS filling with other materials are parameters of the initial PS matrix and the composition of the electrolyte. Deposition of materials in the depth of the porous structure occurs only when the conductivity of silicon crystallites is small enough, i.e. at high porosity of PS. Obtained PS/Ni nanocomposites showed strong anisotropy of magnetic properties and can be used in perspective magnetic sensor and data storage devices. PS/ZnO nanocomposites have high photoluminescence intensity in the visible range which is making them useful for optoelectronic applications.

REFERENCES

1. *Handbook of Porous Silicon* (Ed. L. Canham) (Switzerland: Springer: 2014).
2. R. Herino, *Mater. Sci. Eng., B* **69-70**, 70 (2000).
3. P. Granitzer, K. Rumpf, *Materials* **3**, 943 (2010).
4. *Nanowires: Synthesis, Electrical Properties and Uses in Biological Systems* (Ed. L.J. Wilson) (New York: Nova Science Publishers: 2014).
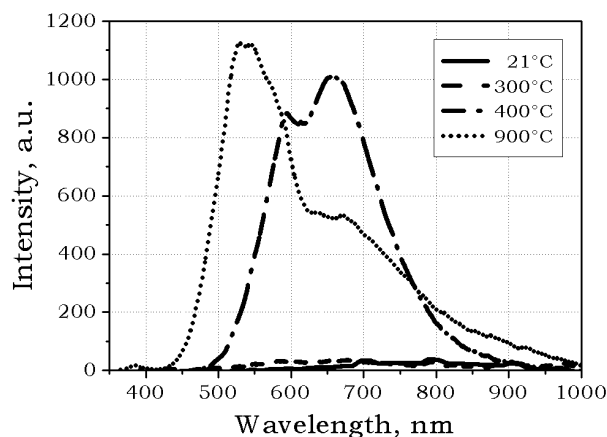5. S. Aravamudhan, K. Luongo, P. Poddar, H. Srikanth, S. Bhansali, *Appl. Phys. A* **87**, 773 (2007).

6. A.L. Dolgiy, S.V. Redko, I. Komissarov, V.P. Bondarenko, K.I. Yanushkevich, S.L. Prischepa, *Thin Solid Films* **543**, 133 (2013).
7. A. Dolgiy, S.V. Redko , H. Bandarenka, S.L. Prischepa, K. Yanushkevich, P. Nenzi, M. Balucani, V. Bondarenko, *J. Electrochem. Soc.* **159**, D623 (2012).
8. E. Chubenko, A. Klyshko, V. Bondarenko, M. Balucani, A. Belous, V. Malyshev, *Adv. Mat. Res.* **276**, 3 (2011).
9. Ü. Özgür, Ya.I. Alivov, C. Liu, A. Teke, M.A. Reshchikov, S. Doğan, V. Avrutin, S.J. Cho, H. Morkoç, *J. Appl. Phys.* **98**, 041301 (2005).